MODIFICATION OF WALL BOUNDARY CONDITIONS FOR LOW-RE κ-ω TURBULENCE MODELS AIMED AT GRID SENSITIVITY REDUCTION

E. M. Smirnov, D. K. Zaitsev
St.-Petersburg State Polytechnic University
St.-Petersburg, Russia

One of the problems of turbulence modeling in industrial applications is the solution sensitivity to the near-wall grid spacing. The low-Re formulations aimed at full resolution of the viscous sublayer need the first grid point to be positioned very close to the wall (typically, $y^+<1$) whereas the high-Re models with the standard wall functions are applicable at $y^+>30$ (the logarithmic region). Many techniques were suggested in the literature to reduce these grid requirements. In particular, to extend the high-Re models to lower values of y^+, one can apply the scalable wall-function formulation [1,2]. In this approach the first point of a "too fine" grid is treated as if it were at the edge of the viscous sublayer so that the log-law relations remain valid formally. However the viscous sublayer is not actually resolved and this can have a significant effect on the solution, especially at low Reynolds numbers when the sublayer is relatively thick.

A more accurate approach available now in several commercial CFD codes is to use a low-Re turbulence model along with enhanced wall functions that reproduce both the logarithmic region and the viscous sublayer behavior [2,3,4]. This provides a gradual shift of the model between the standard wall function approach and accurate resolving of the viscous sublayer depending on the grid density. A minor drawback of the enhanced wall function formulation is the necessity of specifying the boundary conditions for turbulence characteristics not at the wall but at the first (inner) computational point. This results in non-uniformity of a numerical algorithm and impedes applying the multigrid technique for convergence acceleration.

In the present contribution an attempt is made to modify the boundary conditions for two popular versions of the k-ω turbulence model (those developed by Wilcox [5] and Menter [6]) to be applied directly at the wall. Tuning of the wall boundary conditions is carried out via computing the canonical Couette flow. To evaluate the proposed modification a series of test computations is performed. A comparison with results obtained on the base of the enhanced wall function technique is presented as well.

Mathematical Formulation

Enhanced wall functions

The standard wall functions utilize the relations established for the logarithmic region of near-wall turbulent flows [7]:

$$u_{\log} = \frac{u_\tau}{\kappa}\log\left(Ey^+\right),\quad u_\tau = \sqrt{\frac{\tau_w}{\rho}}\ ,\ y^+ = \frac{u_\tau y}{\nu} \qquad (1)$$

$$k_{\log} = \frac{u_\tau^2}{\sqrt{C_\mu}}\ ,\quad \omega_{\log} = \frac{u_\tau}{\kappa y\sqrt{C_\mu}} \qquad (2)$$

Assuming that the first computational node is positioned within the logarithmic region (y^+>30), one can use (1) to evaluate the characteristic velocity, u_τ (and, hence, the skin friction, τ_w) from the first-node velocity, while the first-node values of the turbulence characteristics are given by (2). However for a finer grid with the first node falling into the viscosity-affected zone of the flow (the viscous sublayer or the buffer region), relations (1,2) are not valid and, hence, the solution accuracy deteriorates; moreover, a further grid refinement makes the prediction even worse.

A straightforward way for extension of the wall function approach to lower values of y^+ is to apply more general (enhanced) relations that would be valid both in the logarithmic region and in the viscosity-affected zone. Note that these enhanced wall functions should be used along with a low-Re turbulence model that is capable of reproducing the near-wall damping of the turbulence. If so, the model will shift gradually from the standard wall function approach to an accurate resolution of the viscous sublayer depending on the grid density.

For the viscous sublayer where the turbulent viscosity is negligible, one can derive analytically [5,7]:

$$u_{vis} = u_\tau y^+ \qquad (3)$$

$$\omega_{vis} = \frac{6\nu}{\beta y^2}\ ,\quad \beta = 0.075 \qquad (4)$$

As described in [4], simple blending of the log-law relations (1,2) and the viscous sublayer relations (3,4) yields a reasonable approximation of the near-wall profiles that can be employed as enhanced wall functions

$$u \approx \left(u_{vis}^{-4} + u_{\log}^{-4}\right)^{-1/4} \qquad (5)$$

$$\omega \approx \sqrt{\omega_{vis}^2 + \omega_{\log}^2} \qquad (6)$$

Now (5) is used instead (1) to evaluate the skin friction, while (6) yields the first-node value of ω. Note that, in principle, (5) may be replaced by other approximations of the near-wall velocity profile [8,9,10]. For the k- transport equation the zero flux boundary condition can be applied, as this is correct both for the low-Re limit and the logarithmic region.

Modified wall boundary conditions

As mentioned above, the enhanced wall function formulation employs specifying of the boundary condition for the ω- transport equation not at the wall but at the first (inner) computational point. Sometimes however it is preferable to use values of the turbulence parameters specified directly at the wall as it is done for the original versions of the low-Re turbulence models considered. Both the *k-ω* model by Wilcox [5] and the SST model by Menter [6] involve the wall boundary conditions proposed by Wilcox [5]:

$$k_w = 0 \qquad (7)$$

$$\omega_w = \frac{60\nu}{\beta y_1^2} \qquad (8)$$

where y_1 is the distance from the first computational point to the wall. The Wilcox' boundary condition for the specific dissipation rate, ω, is known to be an artificial/numerical one since analytically ω tends to infinity when approaching the wall, as one can see from (4). Moreover the near-wall profile $\omega(y)$ is not actually resolved in the immediate proximity to the wall because between the 1st and the 2nd computational point the wall distance, y, changes typically by two or three times (for the cell-vertex and the cell-center variable arrangement respectively). In fact the magnitude ω_w given by (8) is simply "a huge value" (ten times the expected first-node value, ω_{vis}) that should provide reasonable behavior of the solution farther from the wall. So one is free to modify this value so that to reduce the grid sensitivity of the solution or/and to extend the model capabilities to higher values of y^+.

We have tuned the wall boundary condition for the ω- transport equation computing the canonical Couette flow at the Reynolds number 10^5 to 10^7. The near-wall velocity profile approximation (5) was used for evaluating the skin friction. Zero turbulent kinetic energy was set at the wall. As a result we propose the following modifications of the wall boundary condition for the ω- equation

the Menter SST model:
$$\omega_w = \frac{30\nu}{\beta y_1^2} \tag{9a}$$

the Wilcox k-ω model:
$$\omega_w = \frac{30\nu}{\beta y_1^2}\cdot\left(1+\frac{y_+^2}{150}\right) \tag{9b}$$

One can see that for the Menter SST model, the original magnitude of ω_w is simply halved. For the Wilcox k-ω model an additional limiter is introduced into the modified boundary condition.

Numerical Tests

To evaluate the proposed modification of the wall boundary conditions a series of two-dimensional test computations have been performed. For each test case several successively refined grids were created and the grid refinement effect on the skin friction was examined; the limit solution at $y^+\to 0$ was obtained via extrapolation. Typically for the finest grid the normalized wall distance, y^+, was below 0.3. The cell-to-cell size ratio was kept below 1.15. Along with testing the proposed wall boundary condition modification, computations with the enhanced wall functions (5,6) were carried out for all the test cases (setting κ=0.41, E=9.0, C_μ=0.09). The results obtained with the two approaches are compared extensively.

All the computations were made using the in-house code SINF developed at the Department of Aerodynamics of the St.-Petersburg State Polytechnic University. It is a steady/unsteady compressible/incompressible Navier-Stokes solver based on the second-order finite-volume spatial discretization using body-fitted block-structured grids and cell-centered variable arrangement. A number of turbulence models are implemented in the code including both RANS (ν_t, k, k-ε, k-ω, v^2f) and hybrid RANS/LES approaches. The code has been well validated in a large series of canonical tests and industrial applications.

For short, the following notation is used in the figures presented below:

SST – the Menter SST turbulence model
WL – the Wilcox low-Re turbulence model
EWF – the enhanced wall function formulation (5,6)
MBC – the proposed modified boundary conditions (5,7,9)

Couette flow

The Couette flow computations were carried out at the Reynolds number ranging from 10^5 to 10^7. For all the regimes a similar effect of the near-wall grid spacing on the solution accuracy was obtained. Typical results of the grid sensitivity analysis for the two turbulence models and different near-wall formulations are illustrated in Fig. 1. As expected, the original low-Re formulation is suitable for y^+<3 only; the solution accuracy deteriorates rapidly when the first computational point moves out of the viscous sublayer. At y^+>20, the Menter SST model gave completely wrong distribution of the eddy viscosity, and the iterations diverged when using the Wilcox model.

The enhanced wall functions yield quite reasonable results at any grids with y^+ ranged from 0.03 to 500. The skin friction coefficient computed deviates from its benchmark ($y^+ \to 0$) value within 11% for the Wilcox model and within 8% for the Menter SST model. Note however that the skin friction is systematically underestimated. A detailed analysis of the solution has shown that specifying the first-node value of ω according to (6) results in excessively high values of ω close to the wall and this, in turn, affects the eddy viscosity and the near-wall velocity distribution. One can see from Fig. 1 (curve 3) that a reduction of the first-node value of ω by 30% improves the prediction considerably.

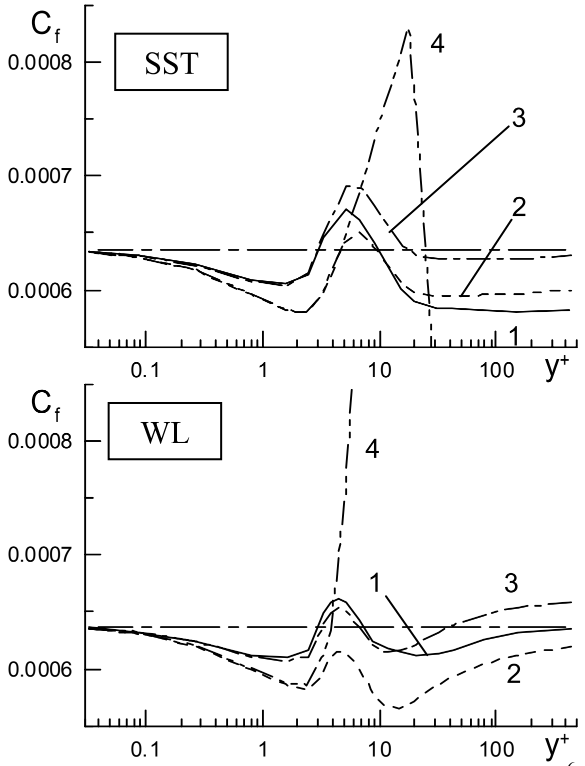

Fig.1. Grid sensitivity test for Couette flow at Re=10^6: 1 – MBC, 2 – EWF, 3 – EWF with ω_1 reduced by 30%, 4 – original low-Re formulation

The results obtained with the modified wall boundary conditions are shown in Fig. 1 with solid lines. As compared to the enhanced wall functions, the new formulation is less grid sensitive for the Wilcox model (deviation of the skin friction from the limit does not exceed 4%). For the Menter SST model the two approaches display similar accuracy (a slight superiority of the modified wall boundary conditions is seen at y^+<10 only).

Fully-developed channel flow

Comparing to the Couette flow, the fully developed channel flow is slightly complicated by the presence of the pressure gradient that has to be adjusted to keep the prescribed flow rate. As well, the channel flow exhibits a less pronounced log-law region.

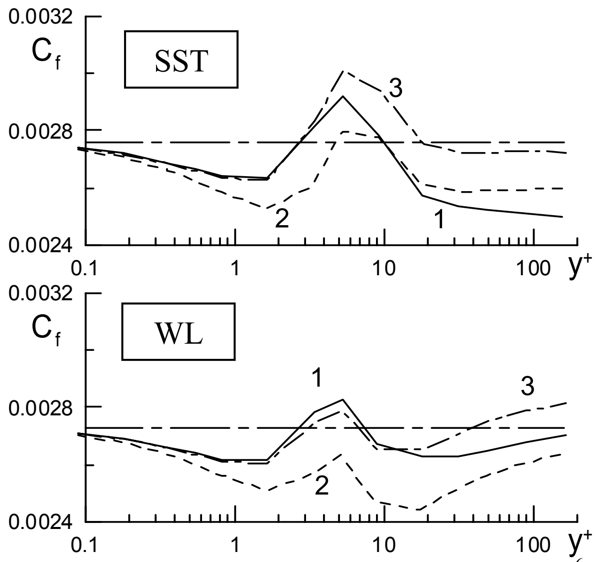

Fig.2. Grid sensitivity test for channel flow at Re=10^6: 1 – MBC, 2 – EWF, 3 – EWF with ω_1 reduced by 30%

The grid sensitivity of the skin friction coefficient computed at Re=10^6 is illustrated in Fig. 2. The results are quite similar to those obtained for the Couette flow. With the Wilcox model the modified wall boundary conditions provide slightly more accurate prediction than the enhanced wall functions (at the most, the skin friction deviates from the limit value by 4% and 10% respectively). With the Menter model both formulations yield the deviation up to 9%. As in the Couette flow case, reduction of the first-node value of ω by 30% improves the accuracy of the enhanced wall function approach.

Flat-plate boundary layer

The flow developing along a flat plate was computed using a non-uniform rectangular grid. Low-turbulence free-stream conditions were specified at the inlet. The Reynolds number based on the plate length was set to 10^7.

Skin friction distributions along the plate computed using different grids are shown in Fig. 3(a); the data presented were obtained with the Wilcox k-ω model and the modified wall boundary conditions, however a similar behavior was observed for all the formulations examined. One can see that coarsening of the grid affects mainly the initial region of the flow and it looks like a shift of the transition zone downstream. In this region the boundary layer is too thin to be resolved on a coarse grid, and grids with y^+>60 are hardly acceptable for the case considered (Re=10^7).

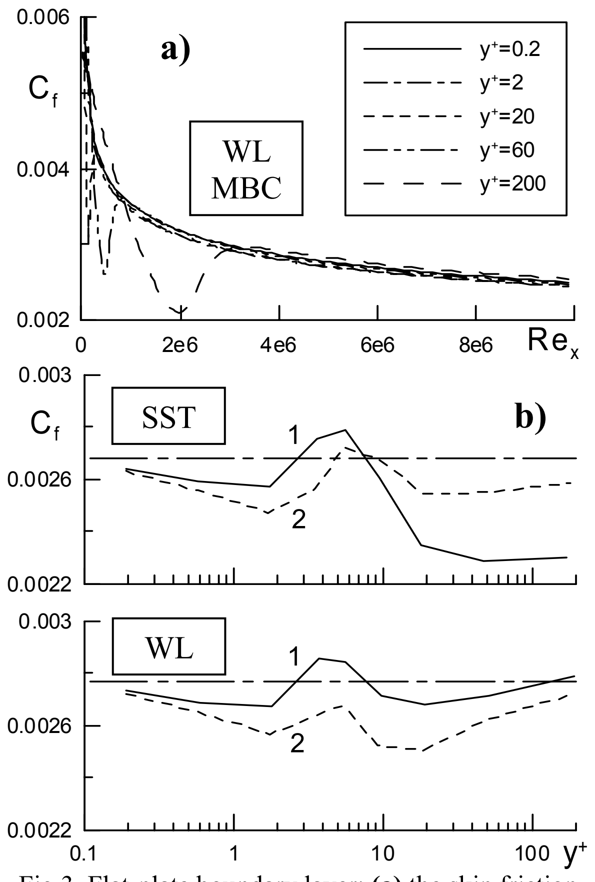

Fig.3. Flat-plate boundary layer: **(a)** the skin friction distribution along the plate and **(b)** the grid sensitivity analysis at Re_x=$8\cdot10^6$ (1 – MBC, 2 – EWF)

Fig. 3(b) shows the skin friction data obtained at Re_x=$8\cdot10^6$. The maximum skin friction deviations from the limit solution are as follows: the Wilcox model with EWF – 10%, with MBC – 4%; the Menter SST model with EWF – 10%, with MBC – 15% (but 4% at y^+<10).

Flow in a turbine blade row

The flow geometry and the computational grid used for computing a turbine cascade flow are illustrated in Fig. 4(a). The pitch equals to 0.78 of the blade chord, the throat is 0.13, the exit flow angle is 80°. For the case considered, the Reynolds number based on the inlet velocity and the chord length was Re=10^6.

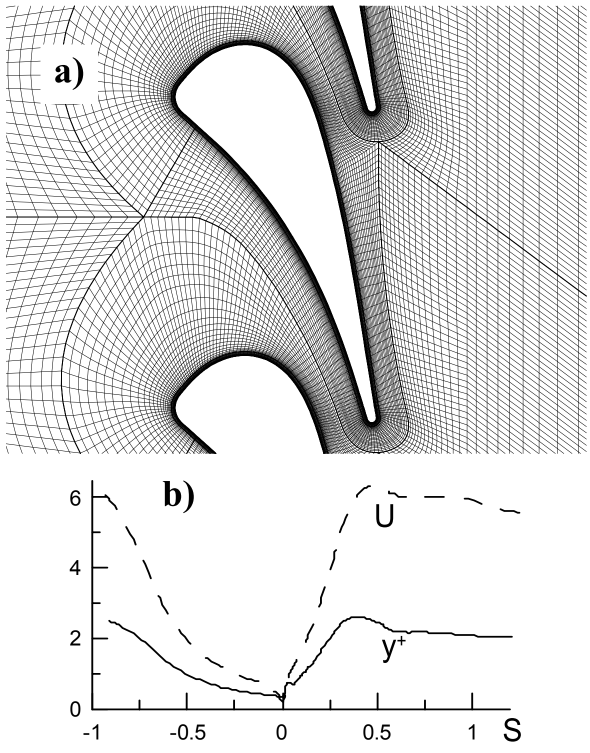

Fig.4. Flow in a turbine cascade: **(a)** the computational grid and **(b)** the pressure-based velocity and a typical distribution of y^+

The diagram in Fig. 4(b) presents a typical y^+ distribution along the surface (close to the wall the grid lines are equidistant); as well, variation of the specific pressure-based velocity (computed from the local pressure via the

Bernoulli law) is shown. One can see that a highly accelerated flow occupies the entire pressure side of the blade and a significant part of the suction side; the y^+ distribution follows the velocity behavior.

Fig. 5(a) shows skin friction distributions along the blade. The solutions obtained using the grids with $y^+ \leq 20$ are quite similar; the grids with typical y^+ values of 50 and 100 produce main deviations in the laminar-turbulent transition region. The solution grid sensitivity at the position S=0.8 is illustrated in Fig. 5(b). The conclusion is same as for the former two flows. The modified wall boundary conditions provide a slightly lower grid sensitivity for the Wilcox model as well as for the Menter SST model at $y^+<10$; at higher values of y^+ the enhanced wall function formulation shows a slightly better performance in case of the Menter model.

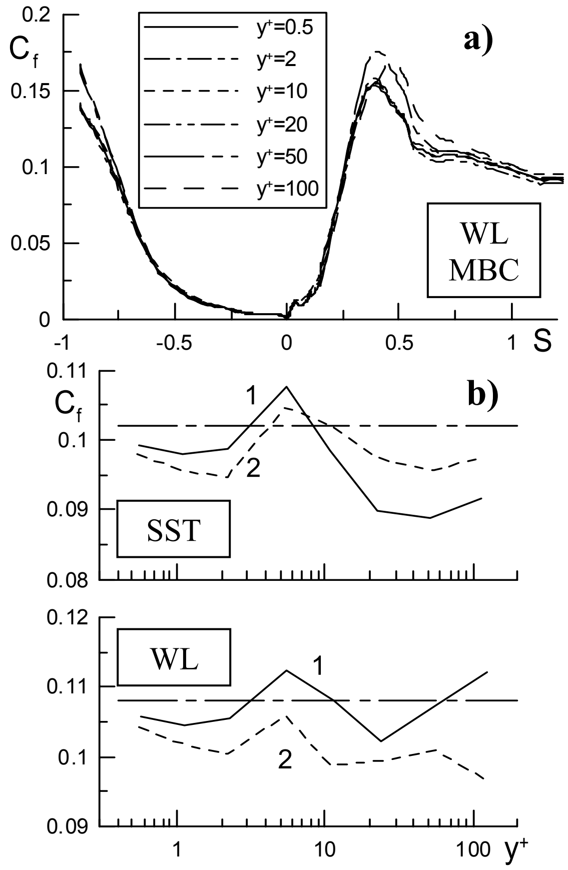

Fig.5. Flow in a turbine cascade: **(a)** skin friction distributions and **(b)** the grid sensitivity test at the position S=0.8 (1 – MBC, 2 – EWF)

Flow past a backward facing step

The flow past a backward facing step involves such complex phenomena as formation of a recirculating zone and the flow reattachment. The flow geometry is sketched in Fig. 6(a). The Reynolds number based on the bulk inlet velocity and the step height was set to $5{\cdot}10^5$. The preceding channel was not included into the computational domain; instead, a power-type velocity profile was specified at the inlet section and the turbulence parameters typical for the fully developed flow in the preceding channel were assigned. Such a simplified formulation of the problem does not provide an adequate modeling of the flow past a backward facing step but it is acceptable for evaluation of the performance of different boundary conditions.

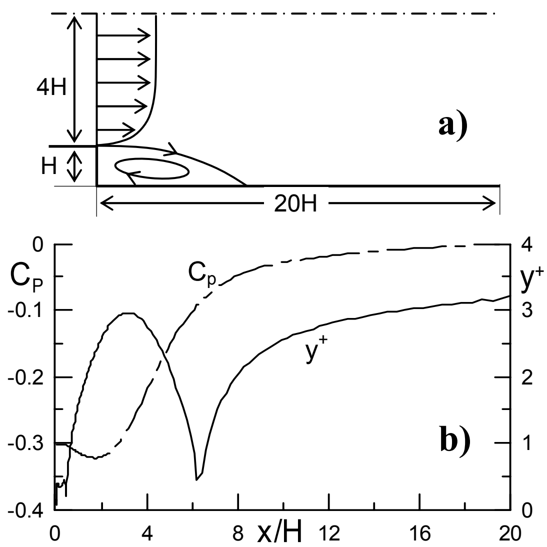

Fig.6. Flow past a backward facing step: **(a)** the flow geometry and **(b)** variation of the pressure coefficient and a typical distribution of y^+

The pressure variation along the wall and a typical distribution of y^+ are shown in Fig. 6(b). The skin friction distributions computed using the Menter SST model with the two formulations examined are presented in Fig.7 (the Wilcox model produced quite similar results). One can see that even for this complicated flow, the two formulations are accurate enough at $y^+<10$ but both of them fail at y^+ exceeding 30.

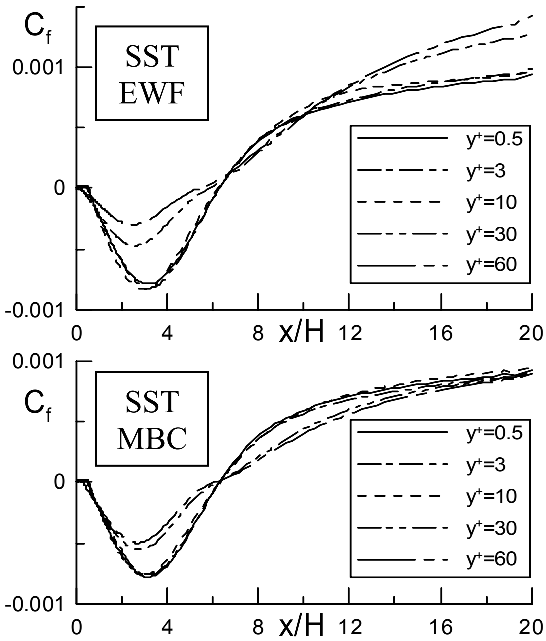

Fig.7. The skin friction distribution past a backward facing step

Conclusions

Modifications of boundary conditions have been proposed for the Wilcox low-Re *k-ω* turbulence model and for the Menter SST model in order to reduce the solution sensitivity to the near-wall grid spacing. The modified wall boundary conditions for the specific dissipation rate are suggested to use in combination with the enhanced wall function technique applied to the momentum equation.

A series of test computations have been performed for different flow configurations to evaluate the performance of the new formulation in comparison with the enhanced wall function method described in [4]. In all the tests considered both approaches have exhibited a good robustness. In terms of the skin friction data, the new formulation was found to be less sensitive to the near-wall grid spacing at any y^+ values for the Wilcox model, and at $y^+<10$ for the Menter model. It has been established also that in case of using the enhanced wall functions, a decrease of the first-node value of the specific dissipation rate by 30% provides a considerable reduction of the grid sensitivity of the solution.

The new formulation of the wall boundary conditions is recommended for implementation into block-structured-grid Navier-Stokes solvers based on the finite-volume spatial discretization technique with the cell-center variable arrangement, and seems to be especially attractive when using the multigrid convergence acceleration.

Acknoledgements

This work was partially supported by the Russian Federation Program for Support of Leading Scientific Schools (grant NSh-1389.2003.8).

References

[1] Grotjans H., Menter F. R. Wall functions for industrial applications. *Computational Fluid Dynamics'98 (Proc. 4th ECCOMAS CFD Conf.),* Vol.1, part 2, pp.1112-1117. John Wiley & Sons, 1998

[2] Menter F. R., Esch T. Elements of industrial heat transfer predictions. *Proc. 16th Brazilian Congress of Mechanical Engineering (COBEM)*, Nov. 2001, Uberlandia, Brazil

[3] Bredberg J., Peng S-H., and Davidson L. On the wall boundary condition for computing turbulent heat transfer with *k-ω* models. *Proc. ASME Heat Transfer division*, Orlando, 2000, pp.243-250

[4] Vieser W., Esch T., and Menter F. R. Heat transfer predictions using advanced two-equation turbulence models. *CFX Validation Report*, CFX-VAL10/0602, 2002, pp.1-73

[5] Wilcox D. C. A two-equation turbulence model for wall-bounded and free-shear flows. *AIAA Paper*, AIAA-93-2905, 1993

[6] Menter F. R. Two-equation eddy-viscosity turbulence models for engineering applications. *AIAA-Journal*, 1994, Vol.32, No.8, pp.269-289

[7] Wilcox D. C. *Turbulence modeling for CFD*. Griffin Printing, Glendale, California, 1993

[8] Kader B. A. Temperature and concentration profiles in fully turbulent boundary layers. *Int. J. Heat Mass Transfer*, 1981, Vol.24, No.9, pp.1541-1544

[9] Huang P., Bradshaw P., and Coakley T. Skin friction and velocity profile family for compressible turbulent boundary layers. AIAA Journal, 1993, Vol.31, No.9, pp.1600-1604

[10] White F., Christoph G. A simple new analysis of compressible turbulent skin friction under arbitrary conditions. *AFFDL Technical Report*, AFFDL-TR-70-133, 1971